

Global Gene Response in *Saccharomyces cerevisiae* Exposed to Silver Nanoparticles

Javed H. Niazi · Byoung-In Sang · Yeon Seok Kim ·
Man Bock Gu

Received: 12 January 2011 / Accepted: 1 March 2011 /
Published online: 16 March 2011
© Springer Science+Business Media, LLC 2011

Abstract Silver nanoparticles (AgNPs), exhibiting a broad size range and morphologies with highly reactive facets, which are widely applicable in real-life but not fully verified for biosafety and ecotoxicity, were subjected to report transcriptome profile in yeast *Saccharomyces cerevisiae*. A large number of genes accounted for ~3% and ~5% of the genome affected by AgNPs and Ag-ions, respectively. Principal component and cluster analysis suggest that the different physical forms of Ag were the major cause in differential expression profile. Among 90 genes affected by both AgNPs and Ag-ions, metalloprotein mediating high resistance to copper (*CUPI-1* and *CUPI-2*) were strongly induced by AgNPs (~45-folds) and Ag-ions (~22-folds), respectively. A total of 17 genes, responsive to chemical stimuli, stress, and transport processes, were differentially induced by AgNPs. The differential expression was also seen with Ag-ions that affected 73 up- and 161 down-regulating genes, and most of these were involved in ion transport and homeostasis. This study provides new information on the knowledge for impact of nanoparticles on living microorganisms that can be extended to other nanoparticles.

Keywords Silver nanoparticles · Nanotoxicity · Microarray · Transcriptome analysis · Yeast genome analysis

Electronic supplementary material The online version of this article (doi:10.1007/s12010-011-9212-4) contains supplementary material, which is available to authorized users.

J. H. Niazi · Y. S. Kim · M. B. Gu (✉)
College of Life Sciences and Biotechnology, Korea University, Seongbuk-gu, Seoul, Republic of Korea
e-mail: mbgu@korea.ac.kr

J. H. Niazi · B.-I. Sang
Center for Environmental Technology Research, Korea Institute of Science and Technology,
Sungbuk-gu, Seoul, Republic of Korea

J. H. Niazi
Faculty of Engineering and Natural Sciences, Sabanci University, Orhanli, Tuzla,
34956 Istanbul, Turkey

B.-I. Sang
Department of Chemical Engineering, Hanyang University, 17 Handang-dong, Sungdong-Ku,
Seoul 133-791, Korea

Introduction

Metal–microbe interactions have been the subject of considerable research attention since last decades, interest has arisen because of the biotechnological potential of microorganisms for metal removal and/or recovery, the possible transfer of accumulated metals to higher organisms in food chains, and the toxicity impacts of metals in nanoparticulate forms toward microbial metabolism and growth; hence, *Saccharomyces cerevisiae* can serve as model microorganisms. Metallic nanoparticles exhibit physical properties that are different from both the ion and the bulk material. This makes them exhibit unique properties such as increased catalytic activity due to morphologies with highly active facets [1, 2]. Nanomaterials, such as nanotubes, nanowires, fullerenes, and quantum dots, have received heavy attentions for their possible enormous applications [3]. Despite of the wide application of these nanomaterials, there is a serious concern regarding the impacts of manufactured nanomaterials on human health and the environment. Studies on nanoparticles have shown that they can pass through biological membranes and affect the physiology of the cell [4]. There have been several reports on the toxicity and risks of nanomaterials in recent years [5–9].

The potential hazard of manufactured nanoparticles (NPs), their release into the aquatic environment, and their harmful effects remain largely unknown [10]. It is also considered that the toxicity test of NPs should be performed in an environmentally relevant mode to avoid misleading information on toxicity of NPs [11]. The effect of NPs on microorganisms is much more extensive and diverse than on plants, invertebrates, and vertebrates [12]. NPs including TiO₂ and Ag have been used as antibacterial agents regardless of the particle sizes, but this activity is enhanced when delivered in nanoparticulate forms. Furthermore, there is insufficient evidence to suggest that all NPs have toxic effects, or in fact that all NPs are toxic to any organisms exposed in an environment. Toxicity assays using specific microorganisms can be used to assess the detrimental effects of various NPs on living organisms and understand their impacts and mode of action. The detailed toxic action of NPs in the cells or interaction with proteins/enzymes, cellular components, and genome responses seems to have been overlooked over the years. A detailed study on a particular type of NPs, impact of size, chemical nature, and genome response to NPs allows elucidating the mode of NP's toxic effects at a molecular and genetic level. Toxicity of NPs can be studied in bacteria and yeast (*S. cerevisiae*) as the model organisms to understand their potential ecological impact.

Currently, two major effects of NPs can be seen and that were studied extensively using bacterial models: (a) cell membrane/cell wall damage and (b) oxidative toxicity by generation of reactive oxygen species. Recently, toxicity of AgNPs in bacteria has been studied using recombinant bacterial biosensors which elucidated the oxidative toxicity of AgNPs compared to microparticles of the same composition [13]. Similarly, studies have also shown the oxidative toxicities of other nanomaterials, such as fullerene, metal oxide NPs including ZnO, CuO, SiO₂, and TiO₂ [12, 14, 15, reviewed in 16]. The toxicity of nanomaterials may vary because of their variable sizes, surface chemistry, or chemical nature of nanomaterials. Likewise, the NPs may also have different effect on different types of cells, which depends on cell wall composition [15]. Therefore, the Scientific Committee on Emerging and Newly Identified Health Risk has suggested that identification of toxicological characteristics of nanomaterials needs to be made on a case-by-case basis [17].

To our knowledge, no genomic response to NPs has been studied. Assessing genomic response to NPs using yeast as a model eukaryote would allow toxicological impacts at

genetic levels. Here we used AgNPs as the model nanomaterials that exhibit a broad size and morphologies with highly reactive facets [5]. Despite of Ag being used as an antimicrobial agent for over a century [18, 19], very little is known on its effect in nanoparticulate form on biological systems. Studies have shown that soluble Ag uses copper transport system in living cells because of structural similarity between copper and Ag [20, 21]. Recently, transcriptome analysis for the response of few metals such as soluble metal ions including silver, which has been shown closely grouped with zinc, was performed [22]. Ag in nanoparticle form may have size-dependent toxicity effects in addition to its bactericidal effects.

In this study, we report on whole genome response to silver in two physical forms (a) nanoparticulate form (AgNPs) and (b) soluble Ag-ions in yeast. Transcriptomes of yeast treated with equimolar mass of silver in these two forms were analyzed. Genes that responded differentially by AgNPs were compared with those that were unique to Ag-ions. Thus, distinct genomic responses can be attributed to the different physical forms of metals.

Materials and Methods

Strain, Media, and Chemicals

S. cerevisiae S288C (α *SUC2 mal mel gal2 CUP1*) was used for all transcriptome analysis and was grown in YPD (1% yeast extract, 2% polypeptone, 2% glucose) at 30 °C. AgNPs were purchased from Nanopoly, Co. (Korea). The AgNPs having a size range 5–10 nm was previously characterized in this laboratory [13] and verified that no agglomeration or aggregation occurred when suspended in YPD medium (Fig. 1).

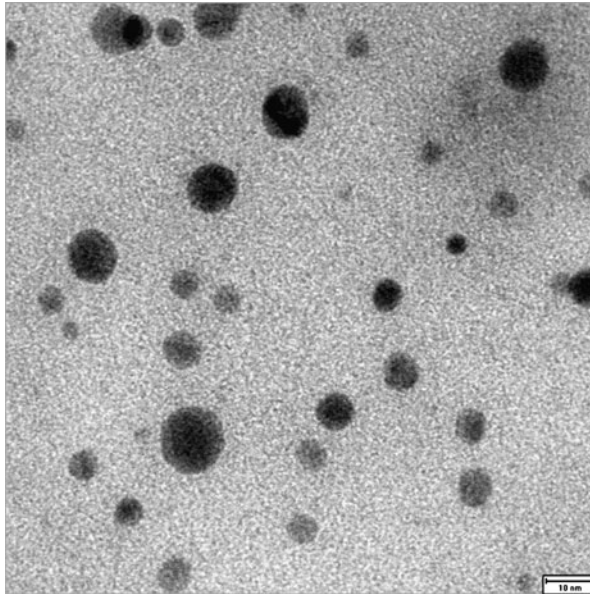


Fig. 1 Transmission electron microscope image of silver nanoparticles suspended in the YPD medium. The nanoparticles measured an average size of ~10 nm

Cytotoxicity Assays

The effect of AgNPs and Ag-ions on cell growth and viability was determined by first diluting an overnight culture of yeast to an optical density of 0.3, at 600 nm, in YPD medium and incubating for different time intervals. To this, different concentrations of equimolar mass of silver in the form of AgNPs or AgNO₃ (Ag-ions) were added and the yeast were incubated at 30 °C, and growth was monitored by observing changes in OD₆₀₀ as a function of time (Fig. S1A and B). The effective concentration of added metal that inhibits by 30% with respect to AgNP concentration was calculated by following Eq. 1

$$I_a = \frac{A_c - A_t}{A_c} \times 100 \quad (1)$$

where I_a is the percent inhibition, A_c is the area under the control growth curve, and A_t is the area under the growth curve at each test concentration. An equivalent Ag mass in the form of AgNO₃ was added for comparison between AgNPs and Ag-ions.

RNA Purification and Microarray Hybridization

For microarray studies, independent yeast colonies were grown overnight in YPD under identical conditions. These cultures were diluted to an OD₆₀₀ of 0.01 and allowed further to grow until till the OD₆₀₀ reaches to 0.3. Cells were then exposed to effective concentration (140 μM) of (a) AgNPs, (b) equimolar concentration of Ag-ions (AgNO₃), and (c) with no metal (control) in YPD. The cells were harvested after 120 and 210 min of incubation at 30 °C, and total RNA was extracted and purified using RNeasy kit (Qiagen). The quality of purified RNA was analyzed spectrophotometrically as well as resolving on a 2% agarose gel. The purified RNA was then stored at -70 °C.

Synthesis of cDNA and Labeling

At least 35 μg of total RNA from treated or untreated samples was added with 0.4 μM oligo-dT primer (QIAGEN) and denatured at 65 °C for 10 min, cooled on ice for 2 min, and the labeled cDNA was synthesized. The reaction mixture contained 0.5 mM each of dATP, dGTP, and dCTP; 0.2 mM dTTP (QIAGEN); 9.5 mM DTT, 15 μM Cy3- or Cy5-labeled dUTP (PerkinElmer Life Science); 1 μL PowerScript Reverse Transcriptase (Clontech); and an appropriate amount of 5× first-strand buffer (Clontech). The reactions were performed at 40 °C for 2 h. The template cDNA was dissolved by the addition of 0.1 N NaOH for 15 min at 65 °C and neutralized by adding 0.1 N HCl. An equal amounts of Cy3- and Cy5-labeled (treated and untreated) cDNA probes solution was mixed and purified using QIA quick PCR purification kit (Qiagen). Hybridization solution was prepared by adding 25 μL of 20× sodium saline citrate (SSC), 10 μL of 0.1% sodium dodecyl sulfate (SDS), 15 μL of formamide, 1 μL of Salmon sperm DNA, and 50 μL of purified labeled cDNA.

Hybridization and Washing of Microarrays

The hybridization solution was applied to Agilent Yeast Oligonucleotide microarrays (Cat. No. G4140B) covered with glass coverslip. The hybridization was carried out at 65 °C for

17–18 h under moist conditions in a hybridization chamber according to manufacturer's instruction. After incubation, the cover-slips were removed by gentle plunging with solution containing $2\times$ SSC and 0.1% SDS (1 min). DNA microarray slides were rinsed twice with solution I ($0.2\times$ SSC and 0.1% SDS) for 3 min, once with solution II ($0.1\times$ SSC and 0.1% SDS) for 5 min, and finally rinsed with solution III ($0.1\times$ SSC) for 1 min. The arrays were then dried by centrifugation at 600 rpm for 30 s. A total of three biological replicates and three reciprocal experiments (dye swap) was performed to avoid dye bias and error analysis.

Scanning and Data Analysis

The hybridized microarrays were scanned with a GenePix 4000B laser scanner (Axon Instrument, Inc., Foster City, CA, USA). Spot validation was performed with GenePix Pro 3.0 software (Axon Instrument, Inc., Foster City, CA, USA) to filter out defective spots which failed to hybridize well during the experimental procedures. For normalization, R language software (version 2.5.1) and “limma” package (version 2.9.1) were used as described previously [23–25]. For functions such as (a) background correction, (b) loess normalization, and (c) scale normalization between arrays were sequentially performed using “limma” package [26]. For the dye swap experiments, the absolute \log_2 ratio value of swapped pairs was averaged with the normal pairs, and the finalized expression set of genes was obtained.

To evaluate significantly expressed genes in triplicate experiments, significance analysis of microarrays (SAM) version 3.02 was used [27], where the response type and the number of permutations were chosen as “one class” and 100, respectively, and all the other options were set to default. Then, non-significant genes, of which false discovery rate from SAM analysis having more than 5%, were filtered out. Finally, only genes whose absolute \log_2 ratios of ≥ 1 or ≤ -1 , which represent up- or down-regulated genes, respectively, in treated samples having at least ≥ 2 -fold differences relative to control in at least one treatment were chosen among 6,263 genes for further analysis.

Principal component analysis (PCA) of the biological replicates was performed using Tanagra 1.4 program [28]. The first three principal components captured over 70% of the variability data. *K*-means clustering on the average fold change in gene expression values was performed with *K*= 3 or 5 for genes. The hierarchical (Euclidean distance and average linking) and *K*-means clustering of the transcriptome was performed using Cluster 3.0 and visualized with Java TreeView 1.14r3 [29, 30]. Gene Ontology (GO) analysis was performed using Gene Ontology mapping, and the group of genes to more general terms and/or bins into broad categories were determined by SGD Gene Ontology Slim Mapper (GO-Slim: Process; *Saccharomyces* Genome Database, Stanford, CA, USA) as well as the Munich Information Centre for Protein Sequences (MIPS) database to classify genes according to their function.

Real-Time RT-PCR

For real-time reverse transcription (RT)-PCR, three primers and probe sets (forward primer, reverse primer, reporter probe) for test genes *CUPI-1*, YHR138C, and *BOP2* and a control *ACT1* gene (Applied Biosystems, USA) were as shown in Table S1. Reporter probes were labeled at the 5' end with the fluorescent reporter dye 6-carboxy-fluorescein (5'-FAM) and the 3'-end with a non-fluorescent quencher. The methods for RT reaction are described in the Supplementary Information section.

Results

Transcriptome analysis of yeast exposed to equimolar mass of Ag in colloidal nanoparticles (5~10 nm size) and soluble ionic (AgNO_3) forms revealed a total of 530 differentially expressed genes at 120 min. The differentially expressed genes by AgNPs and Ag-ions were 191 and 339 genes, respectively. The concentration at which 30% growth inhibition occurred was first determined to be 140 and 46.7 μM for AgNPs and Ag-ions, respectively. Ag-ions severely inhibited the growth of yeast above 46.7 μM of Ag-ions (equivalent to the Ag mass) which was distinct to the growth responses seen in AgNPs exposure. Both AgNPs and Ag-ions inhibited the growth of yeast cells in a concentration-dependent manner (Fig. S1A and B). The growth inhibition occurred during 140 μM of AgNPs exposure, which was similar to that of cells exposed to 46.7 μM of Ag-ions in YPD medium (Fig. S1B). This result demonstrated that Ag in the form of ions was more toxic than the NPs by at least 3-fold. The AgNP concentration at which 30% growth inhibition occurred (140 μM) was chosen for global gene expression studies with Ag-ions as well.

The microarray data points of responses showing consistent results from triplicate and reciprocal experiments were subjected to PCA analysis (Fig. 2). The data included three variables, such as two different exposure times as well as two different forms of Ag (nanoparticulate and ionic forms). The first two components account for over 70% of the variance allowing most of the information to be visualized in two dimensions. An approximate understanding of a class' expression dynamic was obtained quickly by looking at its location in space. For example, genes occupying the lower quadrant (high PCA-1, low PCA-2) are up-regulated early but return to background later in time. These genes have expression levels that decrease over time but maintain a high overall expression level relative to the control [31] (for, e.g., PHO89, HSP12, and HSP26; Fig. 2; Supplementary Table S2). Genes with low overall expression levels that decrease over the course of Ag exposure (irrespective of its physical form) can be found in the lower left quadrant. The genes in the upper right quadrant show overall expression levels that increase over the course of Ag exposure (e.g., CUP1-1 and CUP1-2; Fig. 2; Supplementary Table S2). The differentially expressed genes are clearly distributed, and the PCA suggested that the toxicity of Ag was a major contributing factor in the transcription profile. The genes which showed ≤ 2 -fold expression differences consistently in each condition were compiled. Under normal growth conditions, AgNPs affected the expression of 191 and 189 genes at 120 and 210 min, respectively, after the exposure. While Ag-ions affected the expression of 339 genes at 120 min, the genes affected by AgNPs and Ag-ions were about 3% and 5.4% of the total genome, respectively. The effect of Ag-ions was more pronounced with 170 up- and 169 down-regulated genes, compared to 167 up- and 24 down-regulated genes after the AgNPs exposure (Table 1).

Hierarchical clustering analysis showed tight clustering of genes, and the expression patterns associated with two forms of Ag were considerably different in the distribution of the samples into separate clusters, suggesting similarities in their transcription profiles to colloidal AgNPs, distinct to Ag-ions (Fig. 3). A substantial number of the affected genes were still unknown in their functions, and the largest number of genes affected by AgNPs and Ag-ions was found to be responsive to chemical stimulus, stress, and transport related cellular process (Figs. 2 and 3). Hence, the general toxic effects of AgNPs and Ag-ions appear to be the altered function brought on by genes associated with chemical stimuli, stress, and cellular transport functions (Fig. 3). A noticeably large number of genes involved in cellular rescue and stress response were up-regulated by AgNPs, specifically at early growth stages at 120 min (46 genes) compared to 210 min (37 genes) or Ag-ions

Table 1 Summary of genes affected in *S. cerevisiae* 288C exposed to AgNPs and Ag-ions compared to untreated cells

Experiment	Stress	Exposure time (min)	Genes uniquely affected				Total number of genes affected			
			Up-regulated	Down-regulated	Total	% genome	Up-regulated	Down-regulated	Total	% genome
1	AgNPs	120	17	10	27	0.43	167	24	191	3.052
2	AgNPs	210	5	37	42	0.67	142	47	189	3.02
3	Ag-ions	120	73	161	234	3.74	170	169	339	5.416

copper and cadmium were consistently and strongly up-regulated through 120 to 210 min (~40–45-folds) followed by *GSC2* (encodes for a subunit of 1,3-beta-glucan synthase) and *YSR3* (membrane protein; 4.6-folds; Table S2). It is well documented that the *CUP1-1* and *CUP1-2* are synthesized in response to increased cytosolic copper [32, 33], whereas *GSC2* and *YSR3* (*LBP2*) are responsible for maintaining the integrity of the cell wall and membrane sphingolipids [34–36]. Induction of *GSC2* and *YSR3* particularly after the exposure of AgNP strongly suggests that AgNPs caused cell wall and membrane damages. Out of total 19 genes that were strongly expressed, 12 genes (*PHO89*, *HSP12*, *HSP26*, *HOR7*, *GSC2*, *AMS1*, *CIT2*, *STR3*, *TMA10*, *HSP42*, *RTC3*, and *YBR085C-A* genes)

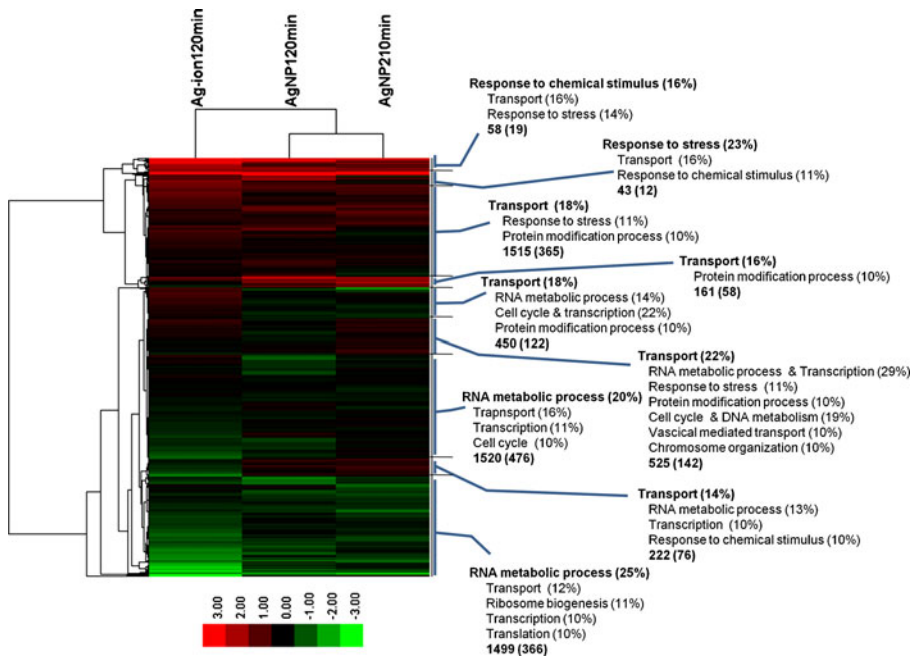


Fig. 3 Hierarchical clustering analysis (Euclidean distance and average linking) of unfiltered expression data of 140 μM Ag elemental mass in the form of NPs (120 and 210 min of treatment) and Ag-ions (120 min of treatment) are indicated above the figure. Gene Ontology mapping (GO-Slim: Process) for the genes and clusters presented in the figure are shown on its right side. The values indicated below the process are the number of genes under each cluster and those in the parenthesis indicating the number of genes with unknown Gene Ontologies. The color scale below the dendrogram extends from -3 to +3 in log₂ space

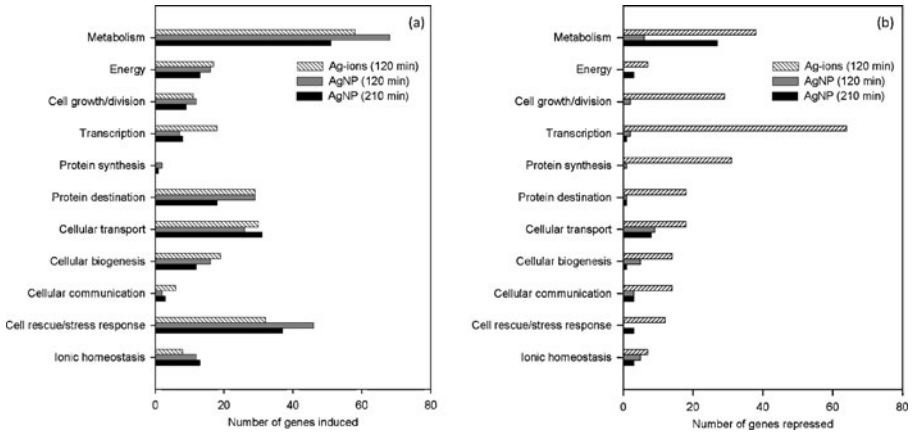


Fig. 4 Effects of silver nanoparticles (AgNPs) and silver ions (Ag-ions) in *S. cerevisiae* 288C after 120 and 210 min of exposure: **a** total number of genes induced to AgNPs and Ag-ions and **b** total number of genes repressed to AgNPs and Ag-ions

dominantly induced at 120 min, while their expression was found to be recovered over time, which was evidenced by declined expression ratios at 210 min (Table S2). PCA and hierarchical clustering placed these genes close together and separated from the others (Figs. 2 and 3). These results suggest that AgNPs severely affected the genes involved in response to vacuolar phosphate transport [37], heat shock [38], hyperosmotic stress, cell wall proteins [39], and metabolism [40] at the early growth stages (120 min).

Conversely, *TIS11*, *CCC2*, *TAF1*, and *FIT2* were moderately expressed at 120 min, but these were found to be highly induced at 210 min of AgNP exposure. These four genes encode cell wall protein as well as transport proteins mainly the Cu^{2+} and iron transporters (Table S3). Further, 16 genes differentially up-regulated at 120 min were found normally expressed at 210 min of AgNPs exposure (Table 1). All these genes were related to metabolism, except *GRX1*, which is responsible for activation to oxidative stress (Table S3) [41]. This result indicated that early exposure of AgNPs caused metabolic imbalance and oxidative toxicity (oxidative stress) in yeast, which is consistent to the effect of AgNPs on high number of genes that take part in cell rescue and stress responses (Fig. 4a). Prolonged exposure with AgNPs (210 min) resulted in uncoupled function of copper and iron transporters, which under normal conditions involved in maintaining Cu^{2+} and iron homeostasis.

Effect of Ag-Ions in Yeast

Exposure of yeast cells with Ag-ions revealed 73 differentially up-regulated and 161 differentially down-regulated genes, which amounts for 3.74% of the total genome (Table 1). Most genes differentially up-regulated by Ag-ions are normally expressed by AgNPs at 120 min exposure (Table S4). However, these genes tend to strongly induced by prolonged exposure of AgNPs through 120 min up till 210 min (Table S4). Further, Ag-ions likely targeted genes responsible for iron retention (*FIT2*), transporter proteins (*SAM3*, *PRM10*, *MEP1*), cell division (*MND1*, *GSP2*), and stress (*GRE3*; Table S4). A total of 90 genes found commonly up-regulated by Ag-ions and AgNPs (Fig. 2). Most strongly up-regulated genes to both AgNPs and Ag-ions are those including *CUP1-1* and *CUP1-2* (mediates resistance to

high levels of copper and cadmium), *PHO89* (Na⁺/Pi cotransporter), and heat shock genes, such as *HSP12* and *HSP26* (Table S2). This result indicated that Ag-ion toxicity was similar to toxicity occurred by AgNPs, but only after 210 min of exposure.

Expression of three candidate genes (*CUPI-1*, YHR138C, and *BOP2*) was selected to validate the microarray results using real-time RT-PCR analysis. The responses of these three genes found in microarray results correlated well with the responses seen with real-time RT-PCR assays (Fig. S2).

Discussion

AgNPs at 120 min of exposure seemed to cause mechanical damage to membrane-bound transport proteins, which resulted into ionic imbalance predominantly with copper and iron after the longer exposure. The fact that highly reactive facets of AgNPs did not have ionic effect at initial growth stages (120 min) suggests that they mainly caused damage to membrane proteins and cell wall. However, at later growth stages (at 210 min), AgNPs appeared to have released ions in the medium, which resulted in the effect similar to that of Ag-ions.

The unfiltered microarray data were initially subjected to PCA and hierarchical clustering analysis that allowed the differentially expressed genes placing close together and separated from the others (Figs. 2 and 3). The severely affected genes by AgNPs were uniquely expressed at 120 min of exposure, and 12 of them were involved in response to vacuolar phosphate transport [37], heat shock [38], hyperosmotic stress, cell wall proteins [39], and metabolism [40]. AgNPs and Ag-ions affected a common set of genes, and notably few of them dominantly induced were related to copper transport and heat shock. Under the normal conditions, increased cytosolic copper activates the copper-sensing transcription factor Ace1p, resulting in the expression of the metallothionein genes *CUPI-1* and *CUPI-2* in yeast (reviewed in [33]). Several copper transporting ATPases have shown to induce by and transport Ag-ions in addition to copper [20, 42, 43]. Ag-ion has no biological significance, and its transport occurs through copper transport system due to the structural similarity, which causes detrimental effect to the cell [20, 21]. Our results showed that exposure of yeast by AgNPs or Ag-ions strongly induced *CUPI-1* and *CUPI-2* genes (Table S2), suggesting that AgNPs or Ag-ions seem to use copper transport system to internalize Ag in to the cell, and as a result *CUPI-1* and *CUPI-2* along with *CCC2* genes were induced strongly to prevent toxicity (Table S2 and S3). Both *CUPI-1* and *CUPI-2* genes are involved in high-level resistance and induction in conditions of excess copper or silver [20, 21, 32, 33, 44], whereas *CCC2* is responsible for pumping copper from cytosol into an extracytosolic compartment and iron uptake [45] and this could be the reason behind their significantly high induction against Ag-ion or prolonged exposure of AgNPs (Table S3).

Nineteen genes were commonly induced to both AgNPs and Ag-ion (Table S2). Out of these, eight genes, such as *PHO89*, *HSP12*, *HSP26*, *AMS1*, *NCE103*, along with three others (*RTC3*, *YDR034W-B*, and *YNL134C*) of unknown function, were strongly induced to colloidal AgNPs at 120 min, compared to those induced to same NPs at 210 min of exposure or with direct Ag-ion exposure (Table S2). The toxic effects of AgNPs or Ag-ions can be related to detrimental effects on the functions associated with these genes. For example, *PHO89* was induced at 120 min but not at 210 min, which is consistent with previous reports that *PHO89* was induced at early growth stages (budding yeast) to phosphate starvation [37, 46], suggesting that AgNPs or Ag-ions influenced efflux of

cellular phosphate, whereas *HSP12* and *HSP26* were induced to changes in osmotic stress [38] and *AMS1* encodes for a vacuolar membrane mannosidase, which is involved in formation of inner surface of the vacuolar membrane [47]. The *NCE103* that commonly induced is regulated by the inorganic carbon (Ci) concentration in the surrounding medium, which is active under oxidative stress conditions [48, 49]. Our result demonstrated that AgNPs or Ag-ions caused osmotic stress followed by damage to vacuolar membrane and oxidative stress. The genes responsible for these toxicities responded quickly after the cells were exposed to AgNPs or Ag-ions (120 min), and their levels were found to be recovered at later stages (210 min).

Furthermore, 20 genes were differentially induced at 120 min in AgNP exposure that were not significantly induced later at 210 min of AgNP exposure (Table S3 and Fig. 3). These 20 genes were identified to involve in metabolism, cellular transport, stress response, and cation homeostasis according to functional categories of MIPS database. These results also indicated that AgNP exposure to yeast resulted in the damage at early growth stages, possibly due to the toxicity caused by osmotic stress, disruption of the Na⁺/Pi-transporter, vacuolar membrane, and response to oxidative stress.

Interestingly, 18 genes specifically induced by AgNPs after prolonged exposure (after 210 min) were also found to be induced by Ag-ions exposure (120 min), but these genes not induced significantly by AgNPs (log₂ ratio= \leq 1- or \leq 2-folds) at 120 min of exposure (Table S4; Fig. 3). Most of these genes induced at 210 min are involved in cellular ion transport ($P = 1.21 \times 10^{-06}$) followed by stress response ($P = 4.93 \times 10^{-04}$), metabolism ($P = 1.17 \times 10^{-03}$), and transcription categories according to MIPS database combined with the order of number of genes induced (Figs. 3 and 4a, b). Only five genes were unique to 210 min of AgNP exposure that were not induced in other two cases (Figs. 2 and 3 and Table 1). Based on this result, it is clear that longer exposure of AgNPs caused the similar effect as that of Ag-ions (Table S4). Additionally, Ag-ion toxicity was more severe than the AgNPs, possibly because soluble Ag-ions may directly interact with the copper ion transport system than insoluble metallic AgNPs. It should be noted that the exposure of AgNPs for genome response analysis was designed for a short exposure time (120–210 min) during which time the NPs were intact (Fig. 1). This can be clearly understood by the fact that growth inhibition with Ag-ions was more severe than with the AgNPs (Fig. S1 and Table 1) as well as induction of genes that engaged in metal ion homeostasis and transport functions.

In addition, Ag-ions repressed greater number of genes compared to AgNPs, and this can be illustrated by inefficiency of transcriptional processes ($P = 6.97 \times 10^{-11}$), metabolism ($P=0.73$), and other cellular functions (Fig. 4b). AgNPs initially were in the form of intact nanoparticles in the medium, which later appeared to have released the Ag-ions and therefore a common set of genes induced to both AgNPs and Ag-ions (Table S4). However, AgNPs specifically affected metabolism and induced stress responses as evidenced by number of genes induced at 120 min, respectively (Figs. 3 and 4a). Taken together, a large number of genes induced to both AgNPs and Ag-ions and our result indicated that early exposure of AgNPs possibly caused mechanical damage due to the highly reactive facets of nanoparticles and size (~10 nm). This is because *HSP12*, *HSP26*, *GSC2*, *YSR3*, and *SSA4* are primarily induced by damage to cell wall, membrane proteins, and heat shock [34–36, 38]. These genes induced more strongly at early growth stages at 120 min with AgNPs exposure compared to their expression levels at 210 min of AgNPs or by Ag-ions. AgNPs themselves induced genes differentially beyond 120 min of treatment and tend to uncouple the function of copper and iron transporters that are involved in Cu²⁺ and iron homeostasis ($P=>10^{-03}$). For example,

CCC2 moderately induced at 120 min (\log_2 ratio=1.3- or 2.4-fold) but it was strongly expressed at 210 min of AgNP exposure (\log_2 ratio=2.2- or 4.6-fold), and this gene is responsible for exporting cytosolic Cu^{2+} into an extracytosolic compartment and facilitates iron uptake [45]. A similar trend was seen with *TIS11*, *TAF1*, and *FIT2* genes that expressed during starvation of iron, iron homeostasis, and iron retention [50–52]. It is clear that NPs initially affect the transport system mainly involved in transport of ions probably through damaging the cell wall integrity combined with uncoupling the cellular metal ion balance. We used the nanoparticulate and soluble ionic forms of Ag in equimolar instead of ecotoxic levels because of the baseline risk, which comes from the amount of silver that is in the environments and the equivalent AgNPs can then add to that risk, whether by facilitating ions' behavior or disrupting cell activity on their own [53].

Conclusion

The present study showed that the physical form of metallic colloidal nanoparticles do have significant impact on the genome and thus the altered behavior of yeast cells. Here, silver in two different physical forms, such as nanoparticles and soluble ionic forms, were tested to study the genomic response in yeast as a model microorganism. It was found that silver nanoparticles induced differential expression of at least 17 genes that are responsive to chemical stimuli, stress, and transport process in addition to the well-known severe impact exhibited by soluble ionic silver. This study demonstrates the impact of nanoparticles has on the genome of yeast as a model eukaryotic microorganism. There is a need to label other metallic nanoparticles that may have detrimental effect on living organisms including humans and in the ecosystem.

Acknowledgments This research was supported by the Ministry of Environment under “The Eco-technopia 21 project” and in part by Institute Research Program of Korea Institute of Science and Technology (KIST), Korea. The authors are grateful for this support.

References

1. Somorjai, G. A. (2004). *Nature*, 430(7001), 730.
2. Doraiswamy, N., & Marks, L. D. (1996). *Surface Science*, 348(1–2), L67–L69.
3. De Wild, M., Berner, S., Suzuki, H., Ramoino, L., Baratoff, A., & Jung, T. A. (2003). *Annals of the New York Academy of Sciences*, 1006, 291–305.
4. Brooking, J., Davis, S. S., & Illum, L. (2001). *Journal of Drug Targeting*, 9(4), 267–279.
5. Morones, J. R., Elechiguerra, J. L., Camacho, A., Holt, K., Kouri, J. B., Ramirez, J. T., et al. (2005). *Nanotechnology*, 16, 2346–2353.
6. Braydich-Stolle, L., Hussain, S., Schlager, J. J., & Hofmann, M. C. (2005). *Toxicological Sciences*, 88(2), 412–419.
7. Ding, L., Stilwell, J., Zhang, T., Elboudwarej, O., Jiang, H., Selegue, J. P., et al. (2005). *Nano Letters*, 5(12), 2448–2464.
8. Borm, P. J., Robbins, D., Haubold, S., Kuhlbusch, T., Fissan, H., Donaldson, K., et al. (2006). *Part Fibre Toxicol*, 3, 11.
9. Van Hoecke, K., Quik, J. T., Mankiewicz-Boczek, J., De Schampelaere, K. A., Elsaesser, A., Van der Meeren, P., et al. (2009). *Environmental Science & Technology*, 43(12), 4537–4546.
10. Moore, M. N. (2006). *Environment International*, 32, 967–976.

11. Oberdorster, E., Zhu, S., Blickey, T. M., McClellan-Green, P., & Haasch, M. L. (2006). *Carbon*, 44, 1112–1120.
12. Oberdorster, G., Stone, V., & Donakson, K. (2007). *Nanotoxicology*, 1, 2–25.
13. Hwang, E. T., Lee, J. H., Chae, Y. J., Kim, Y. S., Kim, B. C., Sang, B. I., et al. (2008). *Small*, 4(6), 746–750.
14. Heinlaan, M., Ivask, A., Blinova, I., Dubourguier, H. C., & Kahru, A. (2008). *Chemosphere*, 71, 1308–1316.
15. Fang, J., Lyon, D. Y., Wiesner, M. R., Dong, J., & Alvarez, P. J. (2007). *Environmental Science & Technology*, 41(7), 2636–2642.
16. Oberdorster, G., Oberdorster, E., & Oberdorster, J. (2005). *Environmental Health Perspectives*, 113(7), 823–839.
17. SCENIHR. (2006). Available at: <http://ec.europa.eu/health/opinions/2/en/nanotechnologies/1-3/9-conclusion.htm>.
18. Guggenbichler, J. P., Boswald, M., Lugauer, S., & Krall, T. (1999). *Infection*, 27(Suppl 1), S16–S23.
19. Kearney, J. N., Arain, T., & Holland, K. T. (1988). *The Journal of Hospital Infection*, 11(1), 68–76.
20. Solioz, M., & Odermatt, A. (1995). *The Journal of Biological Chemistry*, 270(16), 9217–9221.
21. Solioz, M., & Vulpe, C. (1996). *Trends in Biochemical Sciences*, 21(7), 237–241.
22. Jin, Y. H., Dunlap, P. E., McBride, S. J., Al-Refai, H., Bushel, P. R., & Freedman, J. H. (2008). *PLoS Genetics*, 4(4), e1000053.
23. Gentleman, R. C., Carey, V. J., Bates, D. M., Bolstad, B., Dettling, M., Dudoit, S., et al. (2004). *Genome Biology*, 5(10), R80.1–R80.16.
24. Team, R. D. C. R. (2007). *A language and environment for statistical computing*. Vienna: R Foundation for Statistical Computing.
25. Smyth, G. K. (2005). Limma: Linear models for microarray data. In R. Gentleman VC, S. Dudoit, R. Irizarry, & W. Huber (Eds.), *Bioinformatics and computational biology solutions using R and bioconductor* (pp. 397–420). New York: Springer.
26. Smyth, G. K., & Speed, T. (2003). *Methods*, 31(4), 265–273.
27. Tusher, V. G., Tibshirani, R., & Chu, G. (2001). *Proceedings of the National Academy of Sciences of the United States of America*, 98(9), 5116–5121.
28. Zupan, B., & Demsar, J. (2008). *Clinics in Laboratory Medicine*, 28(1), 37–54. vi.
29. Saldanha, A. J. (2004). *Bioinformatics*, 20(17), 3246–3248.
30. De Hoon, M. J., Imoto, S., Nolan, J., & Miyano, S. (2004). *Bioinformatics*, 20(9), 1453–1454.
31. Raychaudhuri S., Stuart J., Altman R. (2000). Principal components analysis to summarize microarray experiments: Application to sporulation time series. In *2000: NIH Public Access* (p. 455).
32. Li, L., & Kaplan, J. (2004). *The Journal of Biological Chemistry*, 279(32), 33653–33661.
33. Winge, D. R. (1998). *Progress in Nucleic Acid Research and Molecular Biology*, 58, 165–195.
34. Parveen, M., Hasan, M. K., Takahashi, J., Murata, Y., Kitagawa, E., Kodama, O., et al. (2004). *The Journal of Antimicrobial Chemotherapy*, 54(1), 46–55.
35. Mandala, S. M., Thornton, R., Tu, Z., Kurtz, M. B., Nickels, J., Broach, J., et al. (1998). *Proceedings of the National Academy of Sciences of the United States of America*, 95(1), 150–155.
36. Skrzypek, M. S., Nagiec, M. M., Lester, R. L., & Dickson, R. C. (1999). *Journal of Bacteriology*, 181(4), 1134–1140.
37. Hurlimann, H. C., Stadler-Waibel, M., Werner, T. P., & Freimoser, F. M. (2007). *Molecular Biology of the Cell*, 18(11), 4438–4445.
38. Varela, J. C., van Beekvelt, C., Planta, R. J., & Mager, W. H. (1992). *Molecular Microbiology*, 6(15), 2183–2190.
39. Kapteyn, J. C., ter Riet, B., Vink, E., Blad, S., De Nobel, H., Van Den Ende, H., et al. (2001). *Molecular Microbiology*, 39(2), 469–479.
40. Graybill, E. R., Rouhier, M. F., Kirby, C. E., & Hawes, J. W. (2007). *Archives of Biochemistry and Biophysics*, 465(1), 26–37.
41. Luikenhuis, S., Perrone, G., Dawes, I. W., & Grant, C. M. (1998). *Molecular Biology of the Cell*, 9(5), 1081–1091.
42. Riggle, P. J., & Kumamoto, C. A. (2000). *Journal of Bacteriology*, 182(17), 4899–4905.
43. Odermatt, A., Krampf, R., & Solioz, M. (1994). *Biochemical and Biophysical Research Communications*, 202(1), 44–48.
44. Butt, T. R., Sternberg, E., Herd, J., & Crooke, S. T. (1984). *Gene*, 27(1), 23–33.
45. Yuan, D. S., Stearman, R., Dancis, A., Dunn, T., Beeler, T., & Klausner, R. D. (1995). *Proceedings of the National Academy of Sciences of the United States of America*, 92(7), 2632–2636.
46. Lenburg, M. E., & O’Shea, E. K. (1996). *Trends in Biochemical Sciences*, 21(10), 383–387.
47. Yoshihisa, T., & Anraku, Y. (1989). *Biochemical and Biophysical Research Communications*, 163(2), 908–915.

48. Amoroso, G., Morell-Avrahov, L., Muller, D., Klug, K., & Sultemeyer, D. (2005). *Molecular Microbiology*, 56(2), 549–558.
49. Gotz, R., Gnann, A., & Zimmermann, F. K. (1999). *Yeast*, 15(10A), 855–864.
50. Protchenko, O., Ferea, T., Rashford, J., Tiedeman, J., Brown, P. O., Botstein, D., et al. (2001). *The Journal of Biological Chemistry*, 276(52), 49244–49250.
51. Haurie, V., Boucherie, H., & Sagliocco, F. (2003). *The Journal of Biological Chemistry*, 278(46), 45391–45396.
52. De Freitas, J., Wintz, H., Kim, J. H., Poynton, H., Fox, T., & Vulpe, C. (2003). *Biometals*, 16(1), 185–197.
53. Lubick, N. (2008). *Environmental Science & Technology*, 42(23), 8617.